

Performance Improvement of Direct-Power-Controlled PWM Converter

Nguyen Van Hung, and Toshihiko Noguchi (Nagaoka University of Technology)

Abstract – This paper describes a theoretical analysis to compose a switching table of the Direct-Power-Controlled (DPC) PWM converter aimed at performance improvement. Feasibility of the analysis has been proven using a newly proposed switching table through various experimental tests as well as computer simulations. According to the results, the proposed system has demonstrated excellent current waveforms with low distortion, high total-input-power-factor and power conversion efficiency of the converter, which reach up to 99.6 [%] and 96.9 [%] at 1.5-kW load, respectively. Consequently, it has been confirmed that the proposed system surpasses the conventional switching-table-based DPC in every aspect of the performance.

Index Terms – Direct power control, switching table, instantaneous active power, instantaneous reactive power, relay control

I. INTRODUCTION

A Direct-Power-Controlled (DPC) three-phase PWM converter requires a switching table to determine the instantaneous switching states of the converter. These switching states correspond to manipulated variables of the controller to govern the instantaneous active and reactive powers at the same time. Since the DPC is based on relay control of the powers, it is significant to investigate a relationship between the controlled variables, i.e. the powers, and the manipulated variables. There has not been a theoretical background in determining the contents of the switching table where the manipulated variables are stored; hence, a theoretical analysis is absolutely necessary in order to understand how the DPC converter operates.

This paper presents a theoretical analysis to compose a switching table aimed at improving the performance and proves feasibility of the converter using a newly composed switching table through various experimental tests as well as computer simulation tests. According to the test results, the proposed system has demonstrated excellent current waveforms with low distortion and superior characteristics of conversion efficiency and input power factor compared with the conventional system.

II. BASIC SYSTEM CONFIGURATION AND OPERATION

A block diagram of the DPC system is depicted in Fig. 1, where resistances of the interconnecting reactors and dead-time of the converter are neglected [1], [2]. The phase of the power-source-voltage vector is converted to digitized signals, i.e. θ_n ($n=1, 2, \dots, 12$), by using several comparators. Fig. 2 shows quantized phase sectors and one of them where the power-source-voltage vector exists is detected. Also, the errors of the instantaneous active and reactive powers are similarly converted to digitized signals, i.e. S_p and S_q , by using hysteresis comparators. Since the DPC system is based on relay control of the powers, the powers increase or decrease depending on the outputs of the hysteresis comparators, i.e. if S_p or $S_q = 1$, P or Q increases, while in case of S_p or $S_q = 0$,

P or Q decreases, respectively. Therefore, the errors of the powers can be restricted within the hysteresis bands as long as the manipulated variables are appropriately applied to control the powers. The digitized signals S_p , S_q and θ_n are given to the switching table, in which the switching states S_a , S_b and S_c of the converter are stored as shown in TABLE I or II.

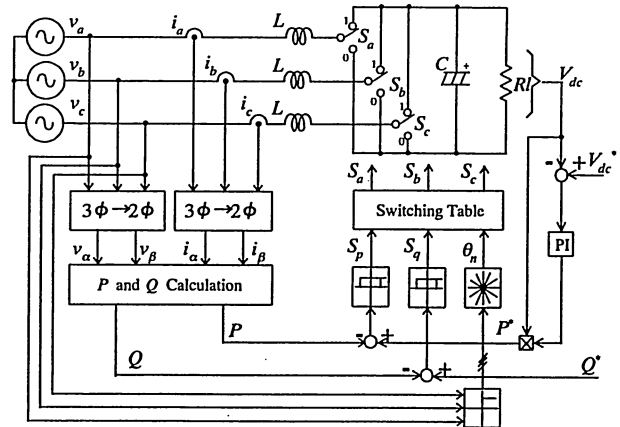


Fig. 1. Block diagram of direct-power-controlled PWM converter.

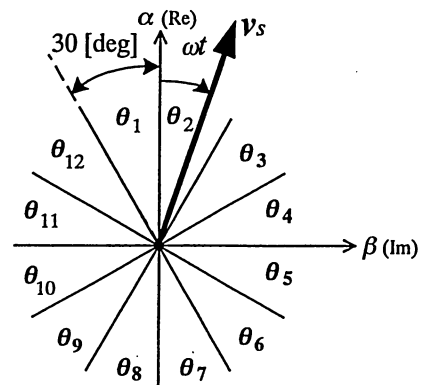


Fig. 2. Power-source-voltage vector and phase sectors.

III. COMPOSING SWITCHING TABLE

The conventional method to compose the switching table was based on a trial-and-error approach using computer simulations, where concrete gradients of the powers with respect to every possible combination of S_a , S_b , S_c and ωt were examined.

TABLE III shows an example of the simulation results. In the simulations, actual behaviors of P and Q were examined by applying intentionally one of eight switching modes of the converter at every 15 [deg] of the power-source-voltage phase angle. The whole switching table, which has been obtained through the process described above, is shown in TABLE I. If the actual behaviors of P and Q are known in a pair of particular neighboring sectors, for example θ_1 and θ_2 , it is not necessary to try another similar simulation test to determine the appropriate switching states because of periodicity of the switching table. However, there is no theoretical background in determining the most appropriate switching state and in composing the switching table.

In order to give a theoretical background to an algorithm of selecting the most appropriate switching state and of composing the switching table, the following analysis has been discussed. Since the values S_p and S_q are either 1 or 0 corresponding to increase or decrease of P and Q , the polarities of dP/dt and dQ/dt are the most important factors to determine the switching modes of the converter. Therefore, it is indispensable to examine mathematically dP/dt and dQ/dt under various combinations of the switching states S_a , S_b and S_c , and the power-source voltage phase θ_n .

The power source voltage vector v_s can be expressed as follows:

$$v_s = \sqrt{2/3}(v_a + v_b e^{j2\pi/3} + v_c e^{j4\pi/3}), \dots (1)$$

$$\left. \begin{aligned} v_a &= \sqrt{2}V_{rms} \cos \omega t \\ \text{where } v_b &= \sqrt{2}V_{rms} \cos(\omega t - 2\pi/3) \\ v_c &= \sqrt{2}V_{rms} \cos(\omega t - 4\pi/3) \end{aligned} \right\} \dots (2)$$

Substituting (2) into (1), the voltage vector v_s can be obtained as

$$v_s = \sqrt{3}V_{rms} e^{j\omega t}. \dots (3)$$

The converter output voltage vector v_c is expressed as

$$v_c = \sqrt{2/3}V_{dc} (S_a + S_b e^{j2\pi/3} + S_c e^{j4\pi/3}). \dots (4)$$

Since interconnecting reactors links the power source and the converter, a voltage and current equation with respect to the reactor can be expressed as (5):

$$v_s - v_c = L di/dt, \dots (5)$$

where the input current vector is defined as

$$i = i_\alpha + j i_\beta = \sqrt{2/3}(i_a + i_b e^{j2\pi/3} + i_c e^{j4\pi/3}). \dots (6)$$

On the other hand, equations of the instantaneous active and reactive powers, i.e. P and Q , are defined as

$$\begin{bmatrix} P \\ Q \end{bmatrix} = \begin{bmatrix} v_\alpha & v_\beta \\ -v_\beta & v_\alpha \end{bmatrix} \begin{bmatrix} i_\alpha \\ i_\beta \end{bmatrix}. \dots (7)$$

After solving the equations from (3) to (7), the equations of dP/dt and dQ/dt can be derived as (8) and (9), respectively.

TABLE I Conventional switching table.

S_p	S_q	θ_1	θ_2	θ_3	θ_4	θ_5	θ_6	θ_7	θ_8	θ_9	θ_{10}	θ_{11}	θ_{12}
1	0	101	111	100	000	110	111	010	000	011	111	001	000
1	1	111	111	000	000	111	111	000	000	111	111	000	000
0	0	101	100	100	110	110	010	010	011	011	001	001	101
0	1	100	110	110	010	010	011	011	001	001	101	101	100

TABLE II Proposed switching table.

S_p	S_q	θ_1	θ_2	θ_3	θ_4	θ_5	θ_6	θ_7	θ_8	θ_9	θ_{10}	θ_{11}	θ_{12}
1	0	001	101	101	100	100	110	110	010	010	011	011	001
1	1	111	111	000	000	111	111	000	000	111	111	000	000
0	0	101	100	100	110	110	010	010	011	011	001	001	101
0	1	100	110	110	010	010	011	011	001	001	101	101	100

TABLE III Simulation results to determine switching state.

Switching State of Converter	Power-source-voltage vector position [ωt]					
	-30 [deg]	-15 [deg]	0 [deg]	15 [deg]	30 [deg]	
111	P	↗	↗	↗	↗	↗
	Q	↗	↗	↗	↗	↗
101	P	↘	↗	↗	↗	↗
	Q	↘	↘	↘	↘	↘
100	P	↘	↘	↘	↘	↘
	Q	↗	↗	↗	↘	↘
110	P	↗	↗	↗	↘	↘
	Q	↗	↗	↗	↗	↗

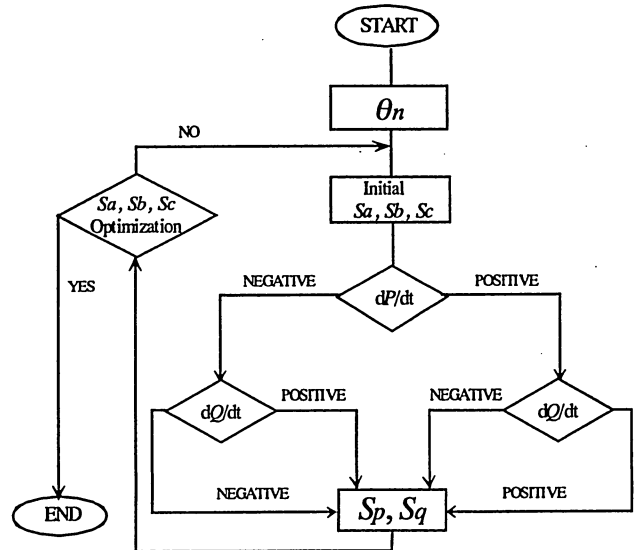


Fig. 3. Algorithm to compose switching table.

$$dP/dt = (\sqrt{2}V_{rms} V_{dc} / L) [(S_a - S_b/2 - S_c/2)(\omega t \sin \omega t - \cos \omega t) - \sqrt{3}/2(S_b - S_c)(\omega t \cos \omega t + \sin \omega t)] \dots (8)$$

$$dQ/dt = (\sqrt{2}V_{rms} V_{dc} / L) [\sqrt{3}/2(S_b - S_c)(\cos \omega t - \omega t \sin \omega t) - (S_a - S_b/2 - S_c/2)(\sin \omega t - \omega t \cos \omega t)] \dots (9)$$

Therefore, it is possible to determine whether the dP/dt and dQ/dt are positive or negative according to every given combination of S_a , S_b , S_c and ωt . A method described in this paper to compose the switching table is based on theoretical values dP/dt and dQ/dt calculated by (8) and (9). If the polarities of dP/dt and dQ/dt are known by substituting S_a , S_b , S_c and ωt into (8) and (9), S_p and S_q can be determined to be either 1 or 0. The flowchart depicted in Fig. 3 shows how to find the optimum switching modes. The proposed switching table obtained through this algorithm is shown in TABLE II.

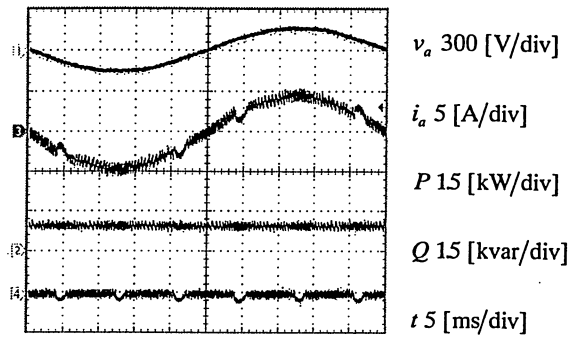
IV. OPERATING CHARACTERISTICS EVALUATION THROUGH EXPERIMENTAL TESTS AND COMPUTER SIMULATIONS

A prototype was implemented to verify feasibility of the proposed switching-table based system. The basic configuration of the prototype is identical to that of Fig. 1, and identical main power circuit and controller were used to make fair comparison between the proposed system and the conventional one. The only difference between them is contents of the switching table. The power circuit of the system consisted of an Insulated-Gate-Bipolar-Transistor (IGBT) based full-bridge circuit. The main electrical parameters of the power circuit and parameters of the controller are given in TABLE IV. An isolation amplifier and two Hall-effect CT's are employed to detect the DC-bus voltage and the line currents, respectively.

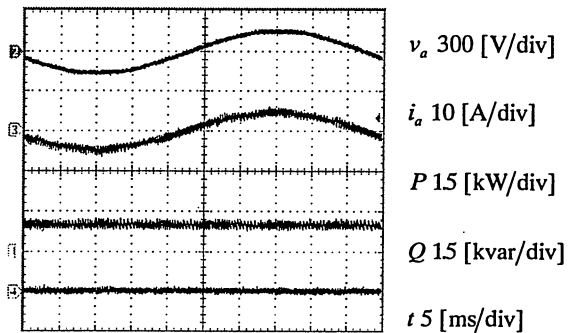
The measured waveforms at 1-kW load are shown in Fig. 4, which are the phase voltage, line current, active power and reactive power waveforms. From these waveforms, it can be seen that the conventional switching-table based system generates reactive power ripple, which results in the current waveform distortion. This reactive power ripple was caused by inappropriate selection of the manipulated variables, i.e. the switching states, to control the powers. However, the system using the proposed switching table properly operates with a sinusoidal line current waveform and the reactive power ripple is effectively suppressed. In these experimental tests, the reactive power was controlled to zero to achieve unity-power-factor operation, so the currents are in phase with the power-source voltages as a result. Fig. 5 shows Total Harmonic Distortion (THD) of the line currents at 1-kW load. Compared the proposed system with the conventional one, the THD was improved from 7.79 % to 3.69 %. Fig. 6 shows total power

TABLE IV Electrical parameters of DPC converter

Inductance of interconnecting reactor	3 [mH]
Resistance of interconnecting reactor	0.2 [Ω]
DC-bus smoothing capacitor	4700 [μ F]
Load resistance	90 [Ω]
Line-to-line power-source voltage	200 [V]
Power-source frequency	50 [Hz]
Average switching frequency	8 [kHz]
Hysteresis bands	200 [W, var]
DC-bus voltage command	300 [V]

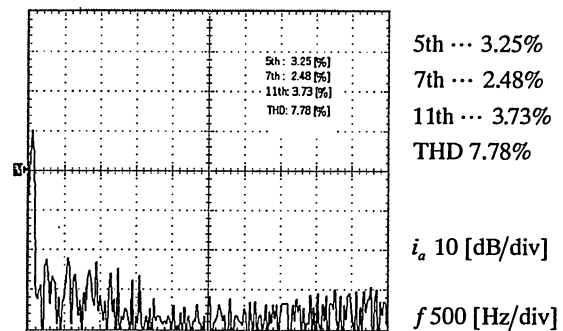


(a) Conventional switching-table based DPC system.

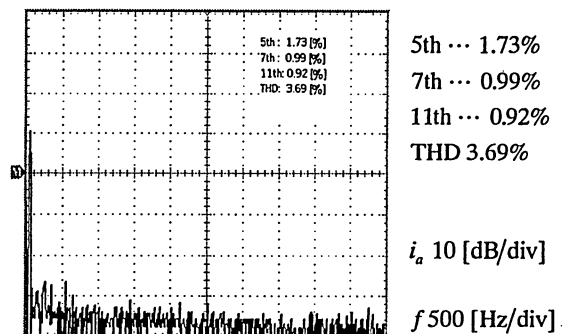


(b) Proposed switching-table based DPC system.

Fig. 4. Operating waveforms of converters.



(a) Conventional switching-table table based DPC system.



(b) Proposed switching-table based DPC system.

Fig. 5. FFT Analysis of line current waveforms.

factor and efficiency of the two systems measured under various conditions of output power. The maximum total power factor and the maximum efficiency of the proposed system were 99.6 % and 96.9 %, respectively. However, they are 99.3 % and 95.8 % for the conventional system. It is clear that the reduced current ripple improved the total power factor and the efficiency of the converter.

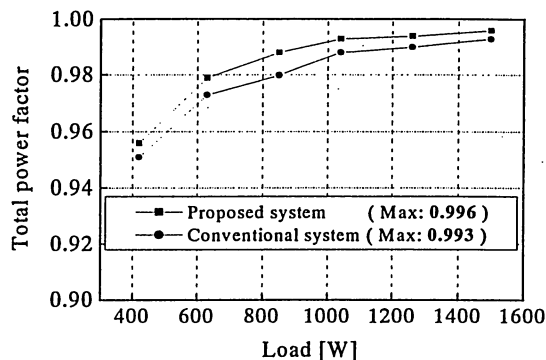
A further performance evaluation has been carried out through computer simulations. It has been known that the reduced capacitor of the converter makes DC-bus voltage unstable. However, the proposed DPC system is applicable to such a condition because it is based on direct relay control of the powers with no current minor loops. The simulations have been conducted under the condition of a 22- μ F DC-bus capacitor to examine the DC-bus voltage controllability and stability. The simulation result is shown in Fig. 7. In this simulation, the DC-bus voltage command was changed stepwise from 300 [V] to 320 [V] and from 320 [V] to 300 [V] under the condition of a 90- Ω load resistance. It can be seen that the proposed system operates with extremely quick response and excellent stability of the DC-bus voltage. Also, it can be confirmed that the input current waveform is sinusoidal with low distortion even though the smoothing capacitor is reduced to 22 [μ F].

V. CONCLUSION

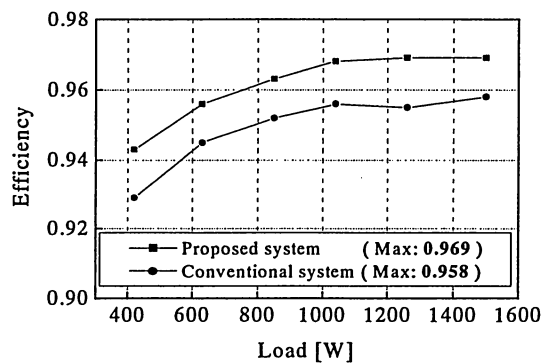
This paper has presented performance improvement of the DPC three-phase PWM converter by using a newly composed switching table, which has been derived on the basis of a theoretical analysis. The theoretical analysis based method makes it possible to select the most appropriate switching state according to the dynamic behaviors of the powers. Also, remarkable improvement of the power and input current waveforms was achieved. Consequently, the total power factor and the conversion efficiency were improved by 0.3 % and by 1.1 % compared with those of the conventional switching-table based system, respectively. Furthermore, according to the computer simulation results, the proposed system demonstrated excellent response and stability of the DC-bus voltage and input current waveforms even though the DC-bus smoothing capacitor was reduced to 22 [μ F].

REFERENCES

- [1] T. Noguchi, H. Tomiki, S. Kondo, and I. Takahashi, "Direct-Power-Control of PWM Converter without Power-Source Voltage Sensors," *IEEE Trans. Ind. Appl.*, vol. 34, no. 3, pp. 473-479, 1998.
- [2] T. Noguchi, H. Tomiki, S. Kondo, and I. Takahashi, and J. Katsumata, "Instantaneous Active and Reactive Power Control of PWM Converter Using Switching Table," *IEEE Trans. Ind. Appl.*, vol. 116-D, no. 2, pp. 222-223, 1996.
- [3] B. R. Lin, Y. L. Hou, and H. K. Chiang, "Implementation of a Three-Level Rectifier for Power Factor Correction," *IEEE Trans. Pow. Elec.*, vol. 15, no. 5, pp. 891-900, 2000.



(a) Total power factor.



(b) Efficiency

Fig. 6. Power factor and efficiency characteristics.

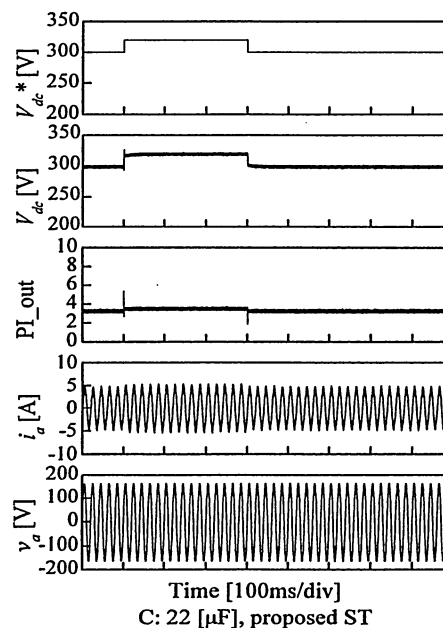


Fig. 7. DC-bus voltage step response at 22- μ F DC-bus smoothing capacitor (simulation).